THE JOURNAL OF BIOLOGICAL CHEMISTRY VOL. 289, NO. 5, pp. 2675–2686, January 31, 2014

Chorismate Pyruvate-Lyase and 4-Hydroxy-3-solanesylbenzoate Decarboxylase Are Required for Plastoquinone Biosynthesis in the Cyanobacterium *Synechocystis* sp. PCC6803

Received for publication, August 23, 2013, and in revised form, December 11, 2013 Published, JBC Papers in Press, December 11, 2013, DOI 10.1074/jbc.M113.511709

Christian Pfaff[‡], **Niels Glindemann**[‡], **Jens Gruber**[‡], **Margrit Frentzen**[‡], **and Radin Sadre**[§1]

From the [‡]*Institute for Biology I, Botany, RWTH Aachen University, Worringerweg 1, 52056, Aachen, Germany and the* [§]*Department of Biochemistry and Molecular Biology, Michigan State University, East Lansing, Michigan 48824*

Background: Plastoquinone biosynthesis in cyanobacteria differs from that in plants.
Results: Chorismate pyruvate-lyase and 4-hydroxy-3-solanesylbenzoate decarboxylase single-gene knock-out mutants are severely affected in plastoquinone synthesis, cell size/structure, and growth.
Conclusion: The plastoquinone biosynthetic pathway likely evolved from a pre-existing ubiquinone pathway in cyanobacterial ancestors.
Significance: Cyanobacterial mutants deficient in plastoquinone biosynthesis allow deeper understanding of processes related to energy transformation.

Plastoquinone is a redox active lipid that serves as electron transporter in the bifunctional photosynthetic-respiratory transport chain of cyanobacteria. To examine the role of genes potentially involved in cyanobacterial plastoquinone biosynthesis, we have focused on three *Synechocystis* sp. PCC 6803 genes likely encoding a chorismate pyruvate-lyase (*sll1797*) and two 4-hydroxy-3-solanesylbenzoate decarboxylases (*slr1099* and *sll0936*). The functions of the encoded proteins were investigated by complementation experiments with *Escherichia coli* mutants, by the *in vitro* enzyme assays with the recombinant proteins, and by the development of *Synechocystis* sp. single-gene knock-out mutants. Our results demonstrate that *sll1797* encodes a chorismate pyruvate-lyase. In the respective knock-out mutant, plastoquinone was hardly detectable, and the mutant required 4-hydroxybenzoate for growth underlining the importance of chorismate pyruvate-lyase to initiate plastoquinone biosynthesis in cyanobacteria. The recombinant Slr1099 protein displayed decarboxylase activity and catalyzed *in vitro* the decarboxylation of 4-hydroxy-3-prenylbenzoate with different prenyl side chain lengths. In contrast to Slr1099, the recombinant Sll0936 protein did not show decarboxylase activity regardless of the conditions used. Inactivation of the *sll0936* gene in *Synechocystis* sp., however, caused a drastic reduction in the plastoquinone content to levels very similar to those determined in the *slr1099* knock-out mutant. This proves that not only *slr1099* but also *sll0936* is required for plastoquinone synthesis in the cyanobacterium. In summary, our data demonstrate that cyanobacteria produce plastoquinone exclusively via a pathway that is in the first reaction steps almost identical to ubiquinone biosynthesis in *E. coli* with conversion of chorismate to 4-hydroxybenzoate, which is then prenylated and decarboxylated.

Plastoquinone (PQ)[2] is synthesized in oxygenic phototrophic organisms only. This prenylquinone plays a central role in photosynthesis. It functions primarily as an electron carrier of the photosynthetic electron transport chain in thylakoid membranes of plants and cyanobacteria where it transfers electrons from the photosystem II reaction center to the cytochrome b_6f complex. Similarly to PQ in thylakoid membranes, ubiquinone functions as a mobile electron carrier in respiratory electron transport chains located in the plasma membrane of most aerobic bacteria and in the inner mitochondrial membranes of eukaryotes. Cyanobacteria, however, possess respiratory electron transport chains in both the plasma and the thylakoid membrane but do not synthesize ubiquinone (1–3). Rather, PQ seems to be the only diffusible prenylquinone in cyanobacterial electron transfer pathways.

The biosynthesis of PQ in plants occurs in the inner envelope membrane of plastids, where a homogentisate solanesyltransferase catalyzes the decarboxylation and the prenylation of homogentisate (4). The reaction product is subsequently methylated at position 3 so that PQ with a solanesyl (nonaprenyl) side chain is formed (5). PQ synthesis in *Synechocystis* sp. PCC 6803 was, in contrast, found to proceed independently of hydroxyphenylpyruvate dioxygenase activity for homogentisate production (6). This suggested that the cyanobacterium uses an alternative or additional pathway for the formation of PQ in comparison to plants. Interestingly, the *Synechocystis* sp. genome was predicted to encode homologs to some of the *Escherichia coli* proteins involved in ubiquinone biosynthesis, which probably contribute to PQ biosynthesis (6). Studies on the biosynthesis and role of PQ in cyanobacteria were, however, prevented by difficulties in generating complete loss of function mutants in candidate genes (1, 7). An *in vivo* labeling approach allowed us to show that *Synechocystis* sp. can use 4-hydroxybenzoate, or a metabolite derived from it, as an aromatic pre-

[1] To whom correspondence should be addressed: Dept. of Biochemistry and Molecular Biology, Michigan State University, East Lansing, MI 48824. Tel.: 517-432-9283; Fax: 517-884-6965; E-mail: sadre@msu.edu.

[2] The abbreviation used is: PQ, plastoquinone.

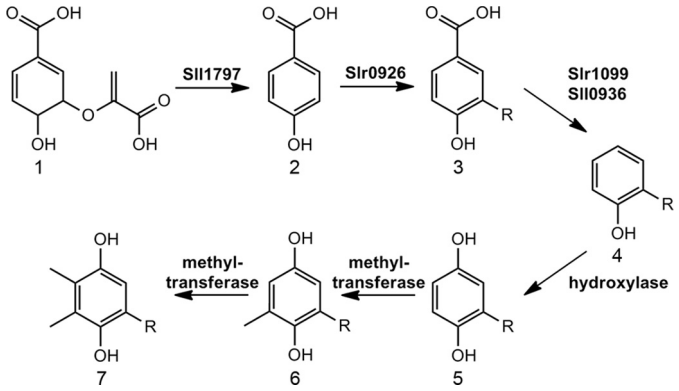

FIGURE 1. **PQ biosynthesis in *Synechocystis* sp. PCC6803.** The chorismate pyruvate-lyase Sll1797 (this study) catalyzes the conversion of chorismate to 4-hydroxybenzoate that is prenylated by Slr0926 (8). Slr1099 (this study) and Sll0936 (this study) are both involved in the decarboxylation of 4-hydroxy-3-solanesylbenzoate. The subsequent reactions are not elucidated. A hydroxylation and two methylation reactions give likely rise to PQ. Sll0418 (5) and some unknown methyltransferases may be involved in the methylation of 2-solanesyl-1,4-benzoquinol to PQ. *1*, chorismate; *2*, 4-hydroxybenzoate; *3*, 4-hydroxy-3-solanesylbenzoate; *4*, 2-solanesylphenol; *5*, 2-solanesyl-1,4-benzoquinol; *6*, 3-methyl-5-solanesyl-1,4-benzoquinol; *7*, plastoquinol; *R*, solanesyl.

cursor for PQ (8). Moreover, we provided evidence for the existence of a membrane-bound aromatic prenyltransferase (Slr0926) in *Synechocystis* sp. that likely catalyzes the prenylation reaction in the PQ biosynthetic pathway similar to respective enzymes involved in ubiquinone biosynthesis (Fig. 1) (8).

The present study is focused on three *Synechocystis* sp. genes, *sll1797*, *slr1099*, and *sll0936*. We show by expression studies in *E. coli*, *in vitro* enzyme assays, and insertional mutagenesis in *Synechocystis* sp. that these genes are required for PQ biosynthesis, where they are involved in the reaction steps before and after the prenylation reaction.

EXPERIMENTAL PROCEDURES

Chemicals—Farnesyl diphosphate and geranylgeranyl diphosphate were obtained from Sigma-Aldrich. [U-^{14}C]4-Hydroxybenzoate with a radiochemical purity of 98% and a specific activity of ~850 dpm/pmol was synthesized by alkali fusion of [U-^{14}C]L-tyrosine (Hartman Analytics) essentially as described (9).

Bacterial Strains and Growth Conditions—Wild type *Synechocystis* sp. PCC6803 was obtained from the Pasteur Culture Collection. The *Synechocystis* sp. cultures were grown photoautotrophically in BG11 liquid medium at 30 °C on an orbital shaker at an photon flux density of 50 μmol·m^{-2}·s^{-1} using a 16-h light/8-h dark cycle (10). *Synechocystis sp.* mutant strains were propagated on BG11 agar plates containing up to 75 μg/ml kanamycin. The optical density of cyanobacterial suspensions was determined at 730 nm (D_{730}) with a photometer.

The *E. coli* insertional mutant strains JW2308–4 (Δ*ubiX*), JW5713–1 (Δ*ubiC*), and the respective wild type BW25113 were obtained from National Bio Resource Project (*E. coli* strain) (11), and AN66 was obtained from Coli Genetic Stock Center (12). The presence of the point mutation (*ubiD420*) in AN66 was confirmed by sequencing. The *E. coli* strains TOP10 (Invitrogen) and BL21AI (Invitrogen) were used for cloning procedures and heterologous expression, respectively. All *E. coli* strains were cultivated under standard conditions in LB medium or in M56 minimal medium (13) supplemented with 30 mM succinate as the sole carbon source. Whenever required, suitable antibiotics were added to the media (50 μg/ml kanamycin, 50 μg/ml carbenicillin, 30 μg/ml chloramphenicol). Growth in *E. coli* liquid cultures was monitored by measuring the increase in optical density at 600 nm (D_{600}). Efforts were made to generate an *E. coli* BW25113 *ubiD* knock-out mutant using essentially the methods described (14, 15).

E. coli Expression Constructs—The open reading frames *sll1797*, *slr1099*, and *sll0936* (16) were amplified by PCR from genomic DNA of *Synechocystis* sp. with the primers sll1797 forward, 5′-AGG ATC CAT GAA GCT TTC TCC GGC CGT TTC C-3′; sll1797 reverse, 5′-AGG ATC CTT ACT CAA ATT TTG GCC TAG GCA ATT C-3′; slr1099 forward, 5′-CTA GAT CTA TGG CAC AAC CTT TGA TTT TGG GGG TC-3′; slr1099 reverse, 5′-CTA GAT CTT CAC TCC CCT TCC ATA CCC CCT TG-3′; sll0936 forward, 5′-CTA GAT CTA TGG CCA GAG ATT TAC GGG GAT TC-3′; and sll0936 reverse, 5′-CTA GAT CTT TAC ACG TCA TAG CCA AAC AAG TTG-3′; and *ubiD* was amplified from genomic DNA of *E. coli* with the primers ubiD F BglII 5′-AG ATC TAT GGA CGC CAT GAA ATA TAA CG-3′ and ubiD R BglII 5′-AGA TCT TCA GGC GCT TTT ACC GTT G-3′. The PCR products were digested with BamHI (*sll1797*) or BglII (*slr1099*, *sll0936*, *ubiD*) and ligated into the pQE60 expression vector (Qiagen) to generate the expression constructs pQE60-sll1797, pQE60-slr1099, pQE60-sll0936, and pQE60-ubiD.

To express Sll1797, Slr1099, and Sll0936 as N-terminal GST fusion proteins in *E. coli* BL21AI, the respective coding sequences were amplified with the primers sll1797 F GW: 5′-CAC CAT GAA GCT TTC TCC GGC CGT TTC C-3′; sll1797 reverse GW, 5′-TTA CTC AAA TTT TGG CCT AGG CAA TTC-3′; slr1099 forward GW, 5′-CAC CAT GGC ACA ACC TTT GAT TTT GG-3′; slr1099 reverse GW, 5′-TCA CTC CCC TTC CAT ACC CCC TTG CCA AC-3′; sll0936 forward GW, 5′-CAC CAT GGC CAG AGA TTT ACG GGG ATT C-3′; and sll0936 reverse GW, 5′-TTA CAC GTC ATA GCC AAA CAA GTT G-3′ and were inserted into the Gateway expression vector pDEST15 (Invitrogen) according to the manufacturer's instructions. The identity of the expression constructs was confirmed by restriction analyses and DNA sequencing.

Complementation Studies in Ubiquinone-deficient E. coli—To determine bacterial growth rates in liquid cultures, the *E. coli* strains BW25113 (wild type) and Δ*ubiC* containing the empty vector as well as Δ*ubiC* with pQE60-sll1797 were grown overnight and then diluted to D_{600} 0.05 in 200 ml of M56 medium supplemented with 30 mM succinate and 50 μg/ml carbenicillin. In contrast, the strains BW25113, Δ*ubiX*/pQE60, and AN66 harboring the empty vector as well as Δ*ubiX* and AN66 containing pQE60-slr1099, pQE60-sll0936, or pQE60-ubiD were cultivated in 200 ml of LB medium with 50 μg/ml carbenicillin and with 1 mM isopropyl β-D-thiogalactopyranoside.

For the determination of the ubiquinone-8 content in *E. coli* cells, overnight cultures were diluted to D_{600} 0.1 in 100 ml of medium. At a D_{600} 0.5, gene expression was induced with isopropyl β-D-thiogalactopyranoside in a final concentration of 1 mM, and cultures were incubated at 37 °C for 3 h. The cultures were centrifuged, and the wet weights of the cell pellets were

determined. Ubiquinone-8 was extracted and analyzed by HPLC essentially as described (8).

Expression Studies in E. coli BL21AI—Heterologous gene expression in *E. coli* cells harboring pDEST15 expression constructs with the *Synechocystis* sp. genes *sll1797*, *slr1099*, and *sll0936* was induced in liquid cultures at a D_{600} 0.6 by addition of L-arabinose (final concentration, 0.2%) to the medium. The cultures were incubated for 2 h at 37 °C, and the cells were then harvested, washed, and disrupted by sonication to prepare crude cell extracts. Subcellular fractions were obtained by differential centrifugation. To this end, the crude cell extract was centrifuged at 5,000 × *g*, and the total protein extract was separated by 100,000 × *g* centrifugation in a soluble and a membrane protein fraction. For immunoblot analyses, the protein samples were separated by discontinuous SDS-polyacrylamide gel electrophoresis and then transferred onto PVDF membranes by semidry blotting. The tagged proteins were immunolabeled with horseradish peroxidase-conjugated GST antibodies (Roche Applied Science). After incubation with LumiLight (Roche Applied Science) substrate, chemiluminescence signals were visualized with a LAS1000 system (Fuji).

Plate Growth Assay and Growth Rates in Liquid Cultures of Synechocystis sp. Mutants—The *sll1797*::*aph*, *slr1099*::*aph*, and *sll0936*::*aph* mutant strains and the wild type were cultivated for 1 week in BG11 liquid medium. Mutant strains were grown in medium supplemented with 50 μg/ml kanamycin. The growth of the mutant strain *sll1797*::*aph* was dependent on the supply with 4-hydroxybenzoate that was added to the BG11 medium to a final concentration of 100 μM. For plate growth assays, the cells were sedimented by centrifugation, washed twice with BG11 medium, and resuspended in BG11 to a D_{730} of 0.1, followed by three 10-fold serial dilutions. Two microliters of each dilution were spotted onto nonselective BG11 agar plates that were incubated at 30 °C for 2 weeks.

The growth rates of *Synechocystis* sp. wild type and mutant strains were determined in BG11 liquid medium. The cultures were inoculated in nonselective BG11 medium to a D_{730} of 0.05, and progress of cell growth was determined by measuring the increase in the D_{730}.

RNA Isolation and Real Time Quantitative PCR—Cells from 10 ml of liquid culture with exponentially growing *Synechocystis* sp. were pelleted by centrifugation at 4 °C and resuspended in 5 ml of TRIzol (17). The cell suspensions were incubated with 500 μl of 1-bromo-3-chloropropane for 10 min. Total RNA was precipitated from the aqueous phase with 1 volume of 2-propanol at 4 °C for 20 min. After centrifugation, the RNA pellets were washed with 70% ethanol (v/v) and resuspended in 100 μl of water. The RNA was treated with DNase (Thermo Fisher) and used as template for first strand cDNA synthesis with AMV RT polymerase (Thermo Fisher) and random hexamer primers. Control reverse transcriptase reactions were performed without enzyme to ascertain that RNA preparations were free from genomic DNA. Aliquots of the cDNA were used as templates for real time quantitative PCR. To carry out real time quantitative PCR, we used a StepOnePlus system (Applied Biosystems), a SYBR green PCR mix (Applied Biosystems), and individual primer pairs (trpA forward, 5′-AGT CCC AGG GCT TTG TTT AC-3′; trpA reverse, 5′-CTT AAC CAT GGC GCT TCC TA-3′; lysC forward, 5′-CCG CAA TTA TGG CAT TCC C-3′; lysC reverse, 5′-TTG GCA ATT TCA AGC CCT AC-3′; 1099 forward, 5′-CAG AAT TTT GGC GCT CTC AG-3′; 1099 reverse, 5′-CCA CCA AGG GTT TAC CTT CT-3′; 0936 forward, 5′-AAC CAA ATC CCC TTG ATC CG-3′; 0936 reverse, 5′-GGC GAT CGC CAC TTC TAA TT-3′; 1797 forward, 5′-CTC CCC CCC AAA TTA ACA CG-3′; and 1797 reverse, 5′-CCG ATT ATG GCC GCA GTA T-3′). The reference genes *trpA* and *lysC* were used to determine fold differences in expression of the target genes *sll1797*, *slr1099*, and *sll0936*.

Purification of Sll1797 GST Fusion Protein—The *E. coli* BL21AI cells harboring the pDEST15 construct with *sll1797* were grown overnight at 37 °C. The next day, 200 ml of LB medium containing 50 μg/ml carbenicillin was inoculated with preculture to a D_{600} of 0.01 and incubated at 37 °C. Gene expression was induced in the bacteria at a D_{600} of 0.6 by addition of 200 μl of 20% L-arabinose to the culture. After 2 h, the cells were harvested, resuspended in 10 ml of 50 mM Bis-Tris propane/HCl, pH 8.0, and subsequently disrupted by sonication. The crude cell extract was centrifuged for 25 min at 9,000 × *g* and 4 °C, and the supernatant was incubated with glutathione-agarose resin (Macherey Nagel) at 4 °C for 15 min in an overhead shaker. The resin was loaded on a column and washed with 10 column volumes of washing buffer (50 mM Bis-Tris propane/HCl, 150 mM NaCl, pH 7.2). Sll1797 GST fusion protein was eluted with 2 column volumes of elution buffer (50 mM Bis-Tris propane/HCl, pH 8.0, 0.4 M NaCl, 50 mM glutathione, 0.1% Triton X-100).

Chorismate Pyruvate-Lyase Assays—Protein extracts were assayed for chorismate pyruvate-lyase activity in 200-μl reaction mixtures containing 50 mM Bis-Tris propane/HCl, pH 8.0, and 450 μM chorismate. After 5 min of incubation at 30 °C, the assays were stopped and extracted with 300 μl of 3 M acetate buffer, pH 4.0, and 500 μl of ethyl acetate containing 2-hydroxybenzoate as an internal standard. The ethyl acetate extracts were subsequently analyzed by HPLC using an Agilent 1100 system with a C18 column (Macherey Nagel) and acetonitrile/water (1:1; v/v) with 0.1% trifluoroacetic acid (v/v) as solvent system at a flow rate of 0.5 ml/min at a wavelength of 255 nm. 4-Hydroxybenzoate and 2-hydroxybenzoate eluted at 8.8 and 15.3 min, respectively. The peak areas of 4-hydroxybenzoate were compared with those of calibration curves. The values for enzymic 4-hydroxybenzoate formation were corrected taking into account that 4-hydroxybenzoate was formed by nonenzymic breakdown of chorismate during assay incubation.

Synthesis of Substrates for Decarboxylase Assays—Radiolabeled 4-hydroxy-3-farnesyl-benzoate and 4-hydroxy-3-geranylgeranylbenzoate were synthesized enzymatically with recombinant Slr0926 as described previously (8). Briefly, *E. coli* membranes containing Slr0926 (20 μg total protein) were incubated in 1-ml reaction mixtures with 50 mM Bis-Tris propane/HCl, pH 7.0, 5 mM magnesium acetate, 50 μM [^{14}C]4-hydroxybenzoate (850 dpm/pmol), and 50 μM prenyl diphosphate at 30 °C for 30 min. The assays were stopped and extracted with 3 ml of chloroform/methanol (2:1, v/v) and 1 ml of 0.9% NaCl solution. Labeled 4-hydroxy-3-octaprenylbenzoate was obtained by incubating *E. coli* Δ*ubiX* mutant cultures with ^{14}C-labeled 4-hydroxybenzoate because Δ*ubiX* accumu-

lates the respective intermediate (18). The cells were harvested, resuspended in 1 ml of water, and disrupted with ceramic beads, and the lipophilic compounds were extracted two times with 10 ml of acetone/petroleum ether (3:2, v/v). The organic phases containing radiolabeled 4-hydroxy-3-prenylbenzoate were collected and dried under a stream of nitrogen gas, and the residues were dissolved in chloroform. The radiochemical purity of the 4-hydroxy-3-prenylbenzoate was analyzed via TLC using a silica gel-coated TLC plate and acetone/petroleum ether (3:7, v/v) as mobile phase and a FLA3000 bioimaging system for detection. The radiochemical concentration of the ^{14}C-labeled 4-hydroxy-3-prenylbenzoate was determined by scintillation counting.

Decarboxylase Assays—The crude cell extracts from *E. coli* containing recombinant *Synechocystis* sp. protein were typically incubated in 400-μl reaction mixtures containing 50 mM Tris-HCl, pH 8.0, and $\sim$ 1 μM 4-hydroxy-3-farnesyl-[U-^{14}C]benzoate or 4-hydroxy-3-geranylgeranyl-[U-^{14}C]benzoate (850 dpm/pmol). The assays were started by the addition of 1.25 mg of protein. After 45 min at 30 °C, prenyllipids were extracted with 800 μl of chloroform/methanol (2:1, v/v) and analyzed via TLC using acetone/petroleum ether (3:7, v/v) as the solvent system. Labeled products were visualized with a FLA3000 bioimaging system and quantified by scintillation counting.

Synechocystis sp. Mutagenesis—To generate disruption cassettes, the *Synechocystis* sp. open reading frames in pQE60 constructs were partially deleted by restriction with AarI (pQE60-sll1797), NaeI and SpeI (pQE60-slr1099), and ClaI and NotI (pQE60-sll0936), and a kanamycin resistance cassette was amplified from pENTR/SD/D-TOPO (Invitrogen) with respective extensions and was inserted into the linearized plasmids. The constructs were used to generate *Synechocystis* sp. gene disruption mutants by homologous recombination (19). Transformants were grown for several plating cycles on BG11 medium containing increasing concentrations of kanamycin to obtain complete segregation. The highest kanamycin concentration was 75 μg/ml. Cultivation media for the *sll1797*::*aph* mutant were supplemented with 100 μM 4-hydroxybenzoate. The complete segregation of the wild type alleles *sll1797*, *slr1099*, and *sll0936* and the respective mutant alleles was confirmed by PCR amplification. In contrast to the PCR products of *sll1797* and *slr1099*, those of *sll0936* were restricted with PvuI prior to electrophoretic analyses to allow univocal identification of wild type and mutated alleles.

Determination of Protein and Chlorophyll Contents—Protein concentrations of total cell extracts were assayed by the Bradford method (20). The chlorophyll contents were determined in 80% acetone according to Lichtenthaler (21).

Oxygen Measurement—*Synechocystis* sp. cells were sedimented from cultures with a D_{730} of 2.0 and resuspended in BG11 medium to a final chlorophyll concentration of 2 μg/ml. The cell suspensions were then transferred into a liquid phase oxygen electrode chamber (Hansatech) and exposed to 50 μmol·m^{-2}·s^{-1} white light. The oxygen evolution rates were measured at 30 °C.

Determination of the Prenyllipid Contents in Synechocystis sp. Mutants—Liquid cultures (25 ml) were grown to a D_{730} of 0.5 and were then incubated with 4 μCi of [U-^{14}C]4-hydroxybenzoate for 5 days. Cells were harvested, washed with water, resuspended in 1 ml of water, and then transferred into a grinding tube. Equal volumes of ceramic beads (Soilgene) and 10 ml acetone/petroleum ether (3:2, v/v) were added for extraction. Cells were disrupted by vortex mixing for 3 min. After phase separation, the petroleum ether phase was collected, and the aqueous phase was re-extracted with 4 ml of petroleum ether. The petroleum ether phases were combined and dried under a stream of nitrogen gas. The residue was dissolved in hexane. PQ and phylloquinone contents in lipid extracts were determined by using an Agilent 1100 HPLC system equipped with a 250/4 Nucleosil 100–5 column (Macherey-Nagel) and 2.2% *t*-butyl methyl ether in hexane as mobile phase at a flow rate of 1 ml/min. Phylloquinone and PQ were detected at 6.9 and 8.2 min, respectively.

RESULTS

In Silico Analyses—In proteobacteria, a chorismate pyruvate-lyase catalyzes the conversion of chorismate to 4-hydroxybenzoate during ubiquinone biosynthesis. Although cyanobacteria do not produce ubiquinone (2, 3), comparative genome analyses led to the prediction of a putative chorismate pyruvate-lyase in some cyanobacteria (22, 7). We performed broader *in silico* analyses on cyanobacterial genomes with PSI-BLAST (23), InterProScan (24), CDD (25), and Delta-BLAST (26). In line with the previous predictions, our analyses indicated that the *Synechocystis* sp. genome carries a single gene, *sll1797*, for a putative chorismate pyruvate-lyase. The open reading frame encodes a small protein with a molecular mass of 16.4 kDa and is annotated as a hypothetical chloroplast open reading frame that belongs to the *ycf21* (hypothetical chloroplast open reading frame) family. Cyanobacterial putative chorismate-lyases are highly divergent in primary sequence (Fig. 2). The predicted ortholog in *Gloeobacter violaceus*, for example, shares only 17% sequence identity with Sll1797. For the *Synechocystis* sp. protein Sll1797, higher sequence identities were determined with homologous proteins of algae such as *Chlorella variabilis* (33% identity) and *Porphyra purpurea* (23% identity), and of plant pathogens, such as the oomycetes of the *Phytophthora* genus, than with the chorismate pyruvate-lyase of *E. coli* encoded by *ubiC* (17% identity) (Fig. 2). In the sequences, an arginine and a glutamate, as well as the spacing between these two amino acid residues, are highly conserved (results not shown). Based on crystal structure data of *E. coli* UbiC (29), Arg-30 and Glu-120 are likely part of the active site of the *Synechocystis* sp. protein. Altogether, the data suggested a role for Sll1797 in aromatic precursor supply for PQ biosynthesis in *Synechocystis* sp. (Fig. 1).

The knowledge on ubiquinone biosynthesis in bacteria is mainly derived from *E. coli* mutant analyses coupled with genetic analyses. It is widely accepted that in *E. coli*, two unrelated proteins, UbiX and UbiD, catalyze the decarboxylation reaction that follows the prenylation of 4-hydroxybenzoate. Like other ubiquinone-deficient mutants, *ubiX* and *ubiD* insertional mutants are impaired in aerobic growth especially in media containing nonfermentable carbon sources (12, 18). Moreover, inactivation of either *ubiX* or *ubiD* alone resulted in the accumulation of the decarboxylase substrate 4-hydroxy-3-

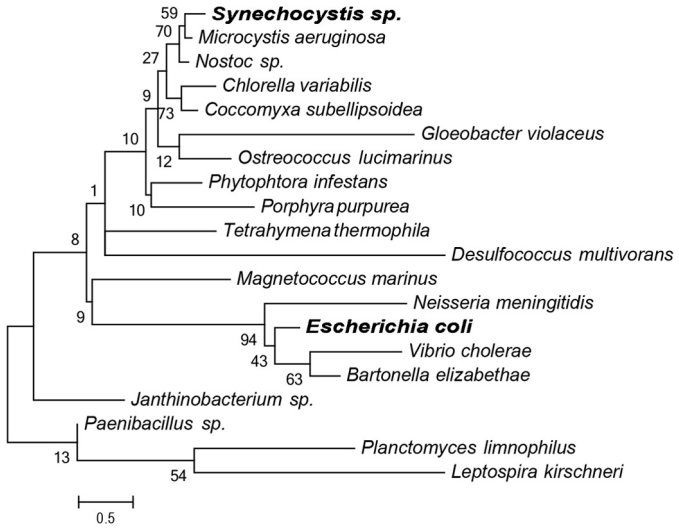

FIGURE 2. **Phylogenetic tree of putative chorismate pyruvate-lyases from different prokaryotic and eukaryotic organisms.** For the phylogenetic tree, sequence alignments were constructed in MEGA 5 using ClustalW (27). The maximum likelihood tree was then generated, and bootstrap values were performed with 500 replications (28). The *scale bar* represents 0.5 amino acid substitutions/site. Note that only the *E. coli* protein UbiC was characterized with regard to its catalytic activity. All analyzed sequences possess two highly conserved amino acid residues, Arg and Glu, which are likely responsible for product coordination (29). The phylogenetic tree is based on the sequences of the following organisms: cyanobacteria: *Synechocystis* sp. PCC6803, NP_440671 (Sll1797); *G. violaceus* PCC 7421, NP_924934; *Microcystis aeruginosa* PCC9701, ZP_18850280; *Nostoc* sp. PCC7107, YP_007049400; proteobacteria: *E. coli* K12, NP_418463 (UbiC); *Vibrio cholerae*, YP_004938445; *Janthinobacterium* sp. CG3, WP_017875115; *Neisseria meningitides*, WP_002240415; *Bartonella elizabethae*, WP_005773162; *Magnetococcus marinus* MC-1, YP_864172; *Desulfococcus multivorans*, WP_020875463; chlorobi: *Chlorobium chlorochromatii* CaD3, YP_380279; PVC group: *Planctomyces limnophilus*, YP_003628196; firmicutes: *Paenibacillus* sp. HW567, WP_019915017; spirochaetes: *Leptospira kirschneri*, WP_016751012; chlorophyta: *Ostreococcus lucimarinus* CCE9901 XP_001421584; *C. variabilis* sp. NC64A, XP_005846790; *Coccomyxa subellipsoidea* C-169, XP_005644772; rhodophyta: *P. purpurea*, NP_053990; oomycota: *Phytophtora infestans* T30-4, XP_002905693; and ciliophora: *Tetrahymena thermophila*, XP_001011395.

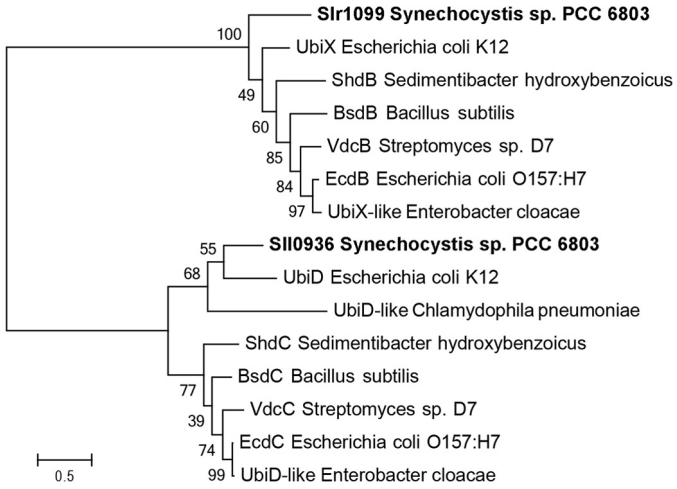

FIGURE 3. **Phylogenetic relationships of the *Synechocystis* sp. proteins Slr1099 and Sll0936 with UbiX- and UbiD-like proteins from bacteria.** The maximum likelihood tree was constructed using MEGA 5 (28). The sequence alignment was conducted in MEGA 5 with Clustal W (27). Bootstrap values were performed with 1000 replications (values shown next to branches). The *scale bar* indicates 0.5 amino acid substitutions per site. With the exception of the *Synechocystis* sp. proteins and the *E. coli* proteins UbiX and UbiD, all other proteins were shown to contribute to 4-hydroxybenzoate decarboxylation *in vitro* (30–34). The reversible multisubunit hydroxyarylic decarboxylases/phenol carboxylases of *Sedimentibacter hydroxybenzoicus*, *Bacillus subtilis*, *Streptomyces* sp. D7, and *E. coli* O157:H7 are encoded by the three clustered genes: B, C, and D. The products of the genes B and C are UbiX- and UbiD-like proteins, respectively. The *Synechocystis* sp. genes *slr1099* and *sll0936* are not clustered: *S. hydroxybenzoicus*, ShdB (AAY67850), ShdC (AAD50377); *B. subtilis*, BsdB (CAB12157), BsdC (CAB12158); *E. cloacae*, UbiX (CAD19476), UbiD (CAD19477); *Streptomyces* sp., VdcB (AAD28781), VdcC (AAD28782); *E. coli*, UbiX (NP_288885), UbiD (NP_418285); *Synechocystis* sp., Slr1099 (NP_440078), Sll0936 (NP_440197); *C. pneumoniae*, UbiD (NP_300323), *E. coli*, EcdB (NP_311620), and EcdC (NP_289287).

octaprenylbenzoate, suggesting that both proteins have decarboxylase activity (12, 18). The *Synechocystis* sp. genome encodes two proteins, Slr1099 (22.2 kDa) and Sll0936 (55.2 kDa), which show 40 and 43% sequence identity to *E. coli* UbiX and UbiD, respectively. They represented, therefore, good candidate enzymes for the third reaction step in the PQ biosynthetic pathway (Fig. 1). Similarly to the *E. coli* proteins, the sequence identity between Slr1099 and Sll0936 is only 12%. Fig. 3 depicts the phylogenetic relationship of Slr1099 and Sll0936 with other members of the UbiX and UbiD like protein families, respectively. These proteins are encoded by many bacterial genomes and have highly conserved sequences. Biochemical data regarding the catalytic activity of UbiX and UbiD like proteins are exclusively limited to aromatic decarboxylases/phenol carboxylases. Direct evidences for enzymatic activity were, so far, provided for UbiD-like proteins from *Chlamydophila pneumoniae* and *Enterobacter cloacae* and one UbiX-like protein from *E. coli* O157:H7 that formed homo-oligomers and catalyzed the decarboxylation of 4-hydroxybenzoate *in vitro* (Fig. 3) (30–34).

Complementation of Ubiquinone-deficient E. coli Mutants by Synechocystis sp. Genes—To investigate the catalytic activity of Sll1797, complementation experiments were performed in an *E. coli* Δ*ubiC* mutant background. Deletion of the *ubiC* gene in *E. coli* leads to reduced growth rates on media with succinate as the sole carbon source because of a severe decrease in ubiquinone content. As given in Fig. 4*A*, expression of the *Synechocystis* sp. gene *sll1797* in the *E. coli* mutant complemented the Δ*ubiC* mutant phenotype despite the very low sequence identities between Sll1797 and UbiC (Fig. 2). The complemented mutant showed growth rates even higher than the wild type control (Fig. 4*A*).

In addition, we tested *slr1099* and *sll0936* for their ability to complement an *E. coli* Δ*ubiX* mutant to gain a first insight into the catalytic activity of these *Synechocystis* sp. proteins. Fig. 4*B* depicts the results from the complementation experiments with the Δ*ubiX* mutant. Although expression of *slr1099* rescued the growth defect of the Δ*ubiX* mutant, no complementation was obtained by expressing the *Synechocystis* sp. *sll0936* gene (Fig. 4*B*) or the *E. coli ubiD* gene (results not shown). The results were further confirmed by the analyses of the ubiquinone content in the *E. coli* mutants (Fig. 4, *C* and *D*). In these experiments, the *E. coli* mutants Δ*ubiC* and Δ*ubiX* expressing *sll1797* and *slr1099*, respectively, accumulated ~80% of the wild type ubiquinone levels.

Because no Δ*ubiD* mutant was available from the Keio collection (11), further complementation experiments were performed in the *E. coli* strain AN66 that carries a point mutation in *ubiD* (2). To our surprise, neither gene expression of *ubiD* nor of *sll0936* or *slr1099* improved the growth rate and the ubiquinone content of AN66 in comparison to mutant cells with an empty vector (results not shown).

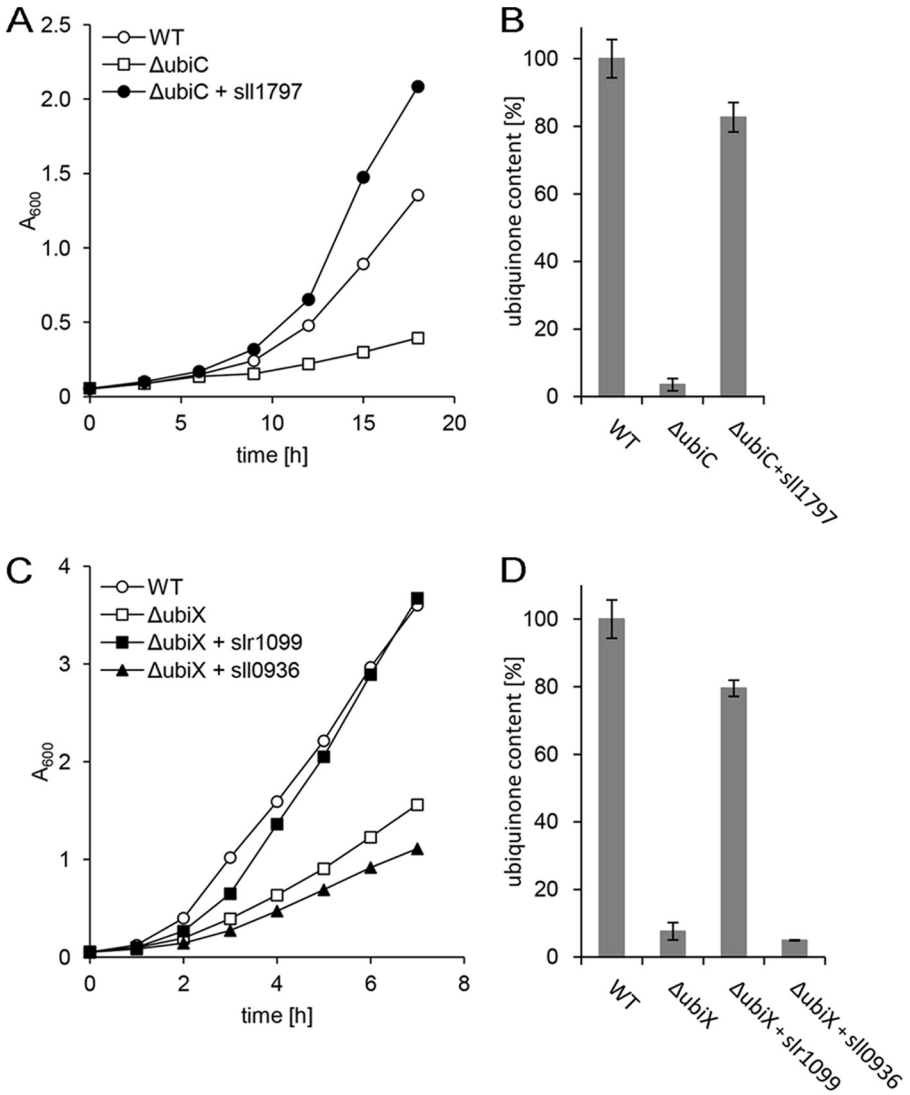

FIGURE 4. **Growth rates and ubiquinone contents of *E. coli* mutants Δ*ubiC* and Δ*ubiX* expressing *Synechocystis* sp. genes.** *A* and *B*, growth rates (*A*) and ubiquinone contents (*B*) of the *E. coli* Δ*ubiC* expressing the *Synechocystis* sp. gene *sll1797* (Δ*ubiC* + *sll1797*) were compared with the WT and the mutant harboring the empty vector. The cells were cultivated in M59 minimal medium supplemented with 30 mM succinate. *C* and *D*, growth rates (*C*) and ubiquinone contents (*D*) of the *E. coli* mutant Δ*ubiX* containing the empty vector or expressing the genes *slr1099* and *sll0936* were determined for cultures grown in LB medium (*A* and *C*). All data are means of at least two independent sets of experiments with S.D. < 0.01. The *error bars* (*B* and *D*) represent S.D. of three independent sets of experiments. 100% ubiquinone is equivalent to ~80 nmol/g of wet weight.

Intensive efforts were therefore made to develop an *E. coli ubiD* knock-out mutant. However, in contrast to Liu and Liu (35), who constructed an *ubiD*::amp mutant strain, we were not able to generate a viable *ubiD* knock-out mutant via insertional mutagenesis. Our results are in line with those of Baba *et al.* (11), who likewise failed to knock out the *ubiD* gene in *E. coli*. These conflicting data suggest that the *ubiD* gene is essential for *E. coli* under certain conditions.

Localization of the Synechocystis sp. Proteins in E. coli—To determine the subcellular localization of the *Synechocystis* sp. proteins in *E. coli*, the recombinant proteins were expressed as GST fusion proteins. Total protein extracts were prepared, separated by high speed centrifugation in a soluble and a membrane protein fraction, and analyzed by SDS-PAGE and Western blotting using an antibody against the GST tag. Fig. 5 depicts results of Western blot analyses. A strong signal was detected for each fusion protein in the 100,000 × *g* membrane fraction, and a very weak signal was detected in the soluble protein fraction (100,000 × *g* supernatant). The data were surprising because none of the *Synechocystis* sp. proteins was predicted to possess typical transmembrane domains (36). Experiments with fusion proteins in which the N-terminal GST sequence was substituted by an N-terminal His epitope gave results similar to those shown in Fig. 5 (results not shown). Treatment of the membrane fractions containing GST-Slr1099 or GST-Sll0936 with high salt concentrations (3 M NaCl or guanidinium thiocyanate) or 1% Triton X-100, for example, did not result in the dissociation of the proteins from the membranes (results not shown).

Attempts to support the subcellular localization of the *Synechocystis* sp. proteins by *in vitro* enzyme assays were successful with regard to the chorismate pyruvate-lyase fusion protein (GST-Sll1797), which showed severalfold higher specific activities in membrane than in soluble protein fractions (Fig. 5*B*).

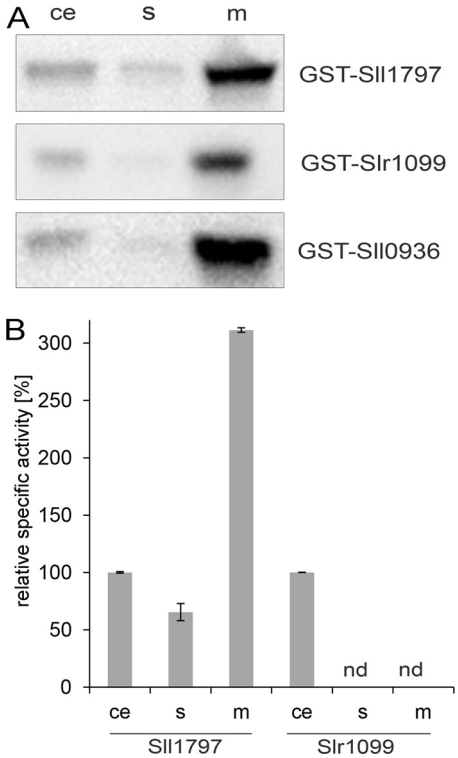

FIGURE 5. **Subcellular localization and enzyme activity of *Synechocystis* sp. proteins expressed in *E. coli*.** *A*, GST-Sll1797, GST-Slr1099, and GST-Sll0936 were expressed in *E. coli* BL21 AI. Proteins of the 5,000 × *g* supernatant (cell extract, *ce*), 100,000 × *g* supernatant (*s*), and 100,000 × *g* sediment fraction (membranes, *m*) were separated by SDS-PAGE and analyzed by immunoblotting with GST antibodies. *B*, the enzyme activities of recombinant Sll1797 and Slr1099 in subcellular fractions of *E. coli* mutant cells Δ*ubiC* and Δ*ubiX*, respectively, are shown. 100% corresponds to relative specific activities of 4.5 μmol·min^{-1}·(μg protein)$^{-1}$ and 1.2 pmol·min^{-1}·(mg protein)$^{-1}$ for Sll1797- and Slr1099-containing fractions, respectively. The *error bars* represent the standard deviations of six independent sets of experiments. *nd*, not detectable; *ce*, 5,000 × *g* supernatant; *s*, 100,000 × *g* supernatant; *m*, 100,000 × *g* sediment.

However, 4-hydroxy-3-prenylbenzoate decarboxylase activity was only detectable in crude protein fractions and only in those containing a Slr1099 protein (Fig. 5*B*).

With the help of glutathione-agarose resin, we succeeded in the purification of the chorismate pyruvate-lyase as GST fusion protein (results not shown). During the purification procedure, the chorismate pyruvate-lyase fusion protein was released from the membranes and behaved like a soluble protein as reported for *E. coli* UbiC (29). Attempts to purify the putative decarboxylases from *Synechocystis* sp. too were not successful.

Enzyme Properties of Sll1797 and Slr1099—The chorismate pyruvate-lyase Sll1797 and the decarboxylase Slr1099 were assayed *in vitro* to determine their enzymatic properties. We used both crude protein extracts and purified GST-Sll1797 fusion protein for these experiments. By removing the enolpyruvyl group from chorismate, Sll1797 produced 4-hydroxybenzoate that was extracted with ethyl acetate from the reaction mixture and analyzed by HPLC. The highest chorismate pyruvate-lyase activities were obtained with 50 mM Bis-Tris propane/HCl at pH 8, 4 mM chorismate, an incubation temperature of 30 °C and an incubation time of 5 min (Fig. 6, *A* and *C*). Under these conditions, reaction rates were constant up to 25 μg of protein (Fig. 6*B*). The Sll1797 activity was not stimulated by divalent cations or, in contrast to the *E. coli* chorismate pyruvate-lyase (37), by increasing the ion strength with NaCl or Bis-Tris propane buffer.

To optimize the conditions for decarboxylase assays, radiolabeled 4-hydroxy-3-prenylbenzoate substrates were synthesized enzymatically as described previously (8) and used as substrates for determining decarboxylase activity. Based on the results depicted in Fig. 5*B*, crude cell extracts from *E. coli* Δ*ubiX* mutant cells expressing *slr1099* were used for these experiments. After assay incubation, chloroform extracts of the reaction mixtures were subjected to TLC analyses as described under "Experimental Procedures." Fig. 7 depicts some properties of the recombinant Slr1099. The *Synechocystis* sp. enzyme catalyzed the decarboxylation of 4-hydroxy-3-prenylbenzoate to 2-prenylphenol *in vitro* and accepted 4-hydroxy-3-prenylbenzoates with different prenyl side chain lengths up to 40 carbon atoms as substrate (Fig. 7*C*). It was slightly more active with 4-hydroxy-3-farnesylbenzoate than with 4-hydroxy-3-geranylgeranylbenzoate (Fig. 7*D*). We did not determine the dependence of Slr1099 on 4-hydroxy-3-octaprenylbenzoate, because this substrate was obtained by *in vivo* labeling with a too low specific activity. The highest Slr1099 activities were obtained at pH 8.5 with 4-hydroxy-3-farnesylbenzoate, an incubation temperature of 30 °C, and an incubation time of 45 min. The addition of divalent cations did not stimulate the Slr1099 activity. Under the optimized assay conditions, no native decarboxylase activity was detectable in protein extracts from *E. coli* Δ*ubiX* cells containing the empty vector. In accordance with the results from complementation experiments (Fig. 4), we were unable to obtain detectable levels of 2-prenylphenols from assays with crude cell extracts from *E. coli* Δ*ubiX* mutant cells expressing *sll0936*.

Characterization of Synechocystis sp. Mutants Deficient in PQ Biosynthesis—To demonstrate that the open reading frames *sll1797*, *slr1099*, and *sll0936* code for proteins involved in cyanobacterial PQ biosynthesis, we inactivated the wild type genes by inserting a kanamycin resistance gene (*aph*) into the open reading frames. The complete segregation of the wild type alleles *sll1797*, *slr1099*, and *sll0936* and the respective mutant alleles was confirmed by PCR amplification (results not shown). In contrast to the PCR products of *sll1797* and *slr1099*, those of *sll0936* were restricted with PvuI prior to electrophoretic analyses to allow univocal identification of wild type and mutated alleles. For each of the three *Synechocystis* sp. mutants DNA fragments of the corresponding mutated alleles were amplified, whereas the shorter wild type fragments were undetectable, suggesting that the mutants were homozygous for the *sll1797*::*aph*, *slr1099*::*aph*, and *sll0936*::*aph* gene disruptions. These results were further validated by analyzing the transcript levels of the three genes in the mutants in comparison to the respective wild type levels by real time quantitative PCR (Fig. 8). The data provided clear evidence that we succeeded in the development of *Synechocystis* sp. single-gene knock-out mutants lacking the chorismate pyruvate-lyase Sll1797, the decarboxylase Slr1099, or the putative decarboxylase Sll0936. Moreover, these results were supported by analyzing the growth rates of the *Synechocystis* sp. mutants. As depicted in Fig. 9*A*, cultivation of the mutated *Synechocystis* sp. strains

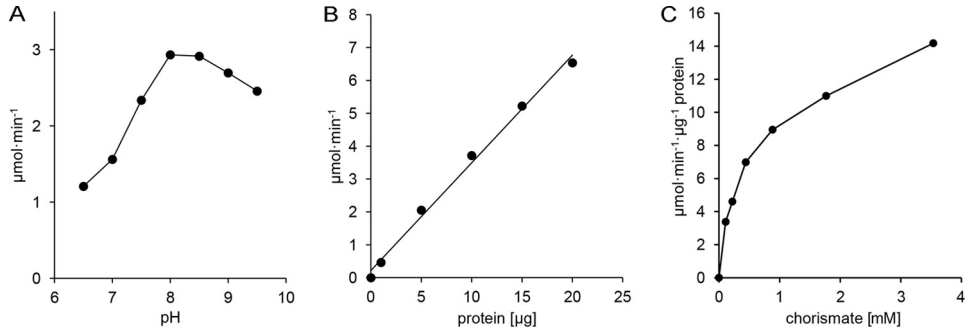

FIGURE 6. **Properties of the recombinant *Synechocystis* sp. chorismate pyruvate-lyase Sll1797.** The dependences on pH (*A*), protein (*B*), and chorismate (*C*) were determined. The assays were carried out in reaction mixtures containing 50 mM Bis-Tris propane/HCl buffer.

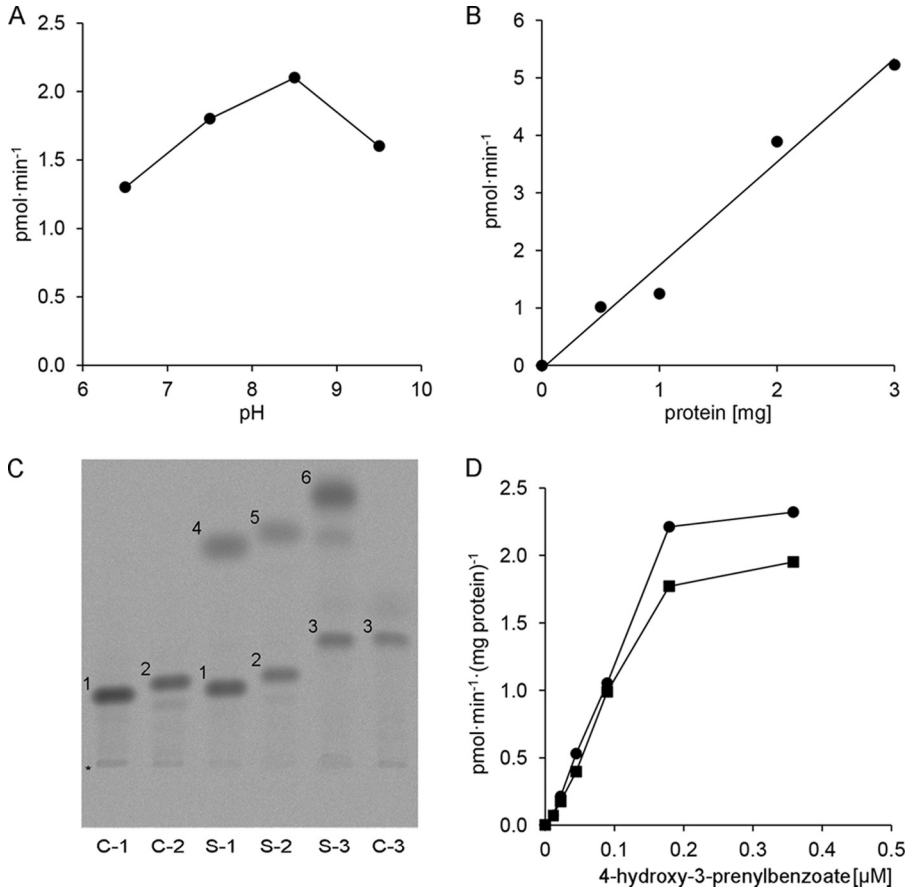

FIGURE 7. **Properties of the recombinant *Synechocystis* sp. decarboxylase Slr1099.** *A* and *B*, the dependences on pH (*A*) and protein (*B*) were determined in assays with 50 mM Bis-Tris propane/HCl buffer and 4-hydroxy-3-geranylgeranylbenzoate as substrate. *C*, Slr1099 (*S-1*, *S-2*, and *S-3*) catalyzed *in vitro* the decarboxylation of 4-hydroxy-3-prenylbenzoates with different prenyl side chain lengths. Control assays (*C-1*, *C-2*, and *C-3*) were conducted with protein extracts from *E. coli* Δ*ubiX* mutant cells harboring the empty vector. *, origin; *1*, 4-hydroxy-3-farnesylbenzoate; *2*, 4-hydroxy-3-geranylgeranylbenzoate; *3*, 4-hydroxy-3-octaprenylbenzoate; *4*, 2-farnesyl-phenol; *5*, 2-geranylgeranyl-phenol; *6*, 2-octaprenyl-phenol. *D*, the dependence on 4-hydroxy-3-prenylbenzoate was determined with 4-hydroxy-3-farnesylbenzoate (*circles*) and 4-hydroxy-3-geranylgeranylbenzoate (*squares*).

under standard growth conditions in BG11 liquid medium resulted in drastically decreased growth rates compared with the parental strain. Under these conditions, the *sll1797*::*aph* mutant showed hardly any growth, but the addition of 4-hydroxybenzoate to the medium rescued the growth defect of the mutant. It showed growth rates even higher than that of the wild type control (Fig. 9*A*). Unlike the *sll1797*::*aph* mutant, both the *slr1099*::*aph* and *sll0936*::*aph* mutant strains were able to grow in BG11 medium but with growth rates distinctly lower than that of the wild type control. Moreover, cultivation of the different strains on BG11 agar plates illustrated the differences in growth rates of *Synechocystis* sp. mutants and wild type strain even more impressively (Fig. 9*B*).

To determine whether the growth rates correlated with the PQ contents in the *Synechocystis* sp. mutant strains, lipid extracts of the cultures were analyzed by HPLC. In line with the lowest growth rate, the *sll1797*::*aph* mutant strain had the lowest PQ content (Table 1). It was nearly 30-fold lower than that of the parental strain. The *slr1099*::*aph* and *sll0936*::*aph* mutants showed growth rates higher than *sll1797*::*aph* but lower than those of wild type cultures consistent with the determined PQ contents (Table 1). These low PQ levels, however, appeared to

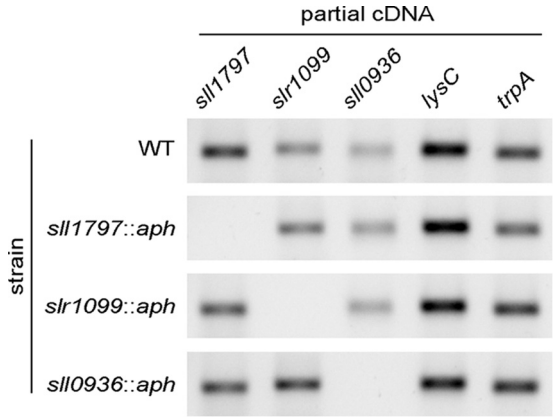

FIGURE 8. **Expression analyses of the developed *Synechocystis* sp. mutant strains.** Partial cDNA sequences were amplified by real time quantitative PCR with gene specific primers from total RNA of *Synechocystis* sp. WT and mutant strains. After 40 PCR cycles, the DNA products were separated by agarose gel electrophoresis. The expression levels were compared with the housekeeping genes *lysC* and *trpA*.

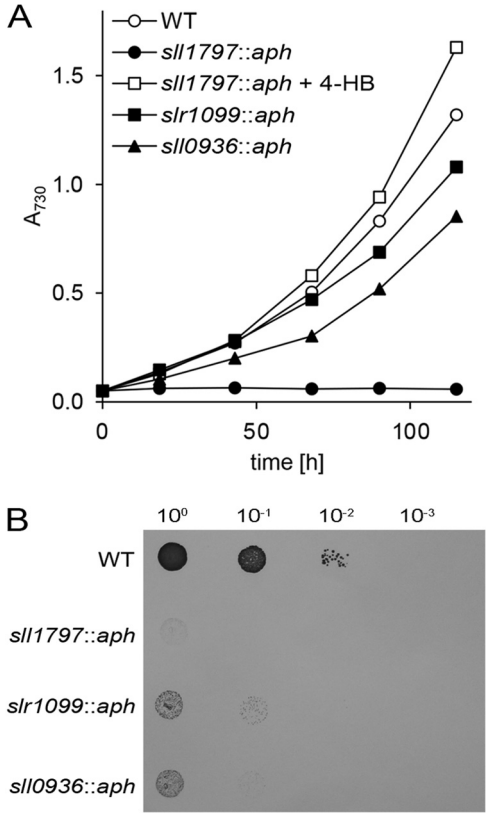

FIGURE 9. ***Synechocystis* sp. gene disruption mutants have severe defects in growth**. *A*, the mutant strains and the WT were cultivated in BG11 liquid medium under standard growth conditions. The growth defect of *sll1797*::*aph* was rescued by the addition of 4-hydroxybenzoate (*4-HB*) to the liquid medium. The final concentration was 100 μM 4-hydroxybenzoate. Mean values of two independent sets of experiments with S.D. < 0.01 are given. *B*, serial dilutions of cultures from the wild type and the *Synechocystis* sp. mutant strains *sll1797*::*aph*, *slr1099*::*aph*, and *sll0936*::*aph* were cultivated on a BG11 agar plate under standard conditions (10^0 corresponds to A_{730} 0.1).

be sufficiently high to sustain photosynthesis rates similar to those of wild type cultures. On the other hand, the very low PQ content of the *sll1797*::*aph* mutant strain was reflected in an extremely weak photosynthesis rate, which comprised ~4% of the wild type only. In contrast to the PQ content, the level of phylloquinone was not affected in the mutants (Table 1). Disruption of one of the three *Synechocystis* sp. genes appeared to influence cell size/structure as reflected by the higher cell numbers/D_{730} ratio, especially in cultures of *sll1797*::*aph* and *sll0936*::*aph* in comparison to the wild type control.

DISCUSSION

Previous studies indicated that cyanobacteria possess an alternative PQ biosynthetic pathway compared with the one in higher plants (6, 8). Here, we continued our studies on *Synechocystis* sp. PCC6803 as a model organism to gain further insight into cyanobacterial PQ biosynthesis. The enzymatic activity and properties of the hypothetical *Synechocystis* sp. protein Sll1797 were investigated. This small protein shares low sequence identities with the *E. coli* UbiC protein, which catalyzes the conversion of chorismate to 4-hydroxybenzoate and pyruvate, the initial step in ubiquinone biosynthesis. Sequence alignment with the sequences of UbiC and different putative chorismate pyruvate-lyases allowed us to predict two conserved amino acid residues (Arg-30 and Glu-120) likely forming part of the active site of Sll1797. The chorismate pyruvate-lyase activity of the *Synechocystis* sp. protein was demonstrated by complementation experiments in an *E. coli* Δ*ubiC* mutant lacking the respective enzymatic activity (Fig. 3) and by *in vitro* enzyme assays with crude and purified enzyme fractions from *E. coli* mutant cells expressing *sll1797* (Figs. 5 and 6). The data were supported and extended by the development and analysis of the *sll1797*::*aph* knock-out mutant of *Synechocystis* sp. The mutant hardly produced any PQ, its photosynthetic electron transport rates were severely impeded (Table 1), and it required 4-hydroxybenzoate, the reaction product of the chorismate pyruvate-lyase, for growth (Fig. 9). Hence, these results provide compelling evidence that the chorismate pyruvate-lyase encoded by *sll1797* catalyzes the initial and essential step in PQ biosynthesis in *Synechocystis* sp.

Although the *Synechocystis* sp. protein Sll1797 possesses no typical transmembrane domains (results not shown), it was largely detected as membrane-associated protein in *E. coli* (Fig. 5). However, membrane association of Sll1797 in *E. coli* appeared to be rather weak, and purification of the recombinant *Synechocystis* sp. protein resulted in a soluble chorismate pyruvate-lyase protein (results not shown). Provided that membrane association occurs also in the native cellular environment, such an interaction can facilitate the transfer of the Sll1797 reaction product to the membrane bound 4-hydroxybenzoate solanesyltransferase, Slr0926, for the second step in the PQ biosynthetic pathway (8) (Fig. 1).

Based on *in silico* analyses, Slr1099 and Sll0936 were selected as candidate proteins that may be involved in the decarboxylation of 4-hydroxy-3-solanesylbenzoate to 2-solanesylphenol (Fig. 1). The *Synechocystis* sp. proteins were identified because of their high sequence similarity to UbiX and UbiD of *E. coli* (12, 18) involved in ubiquinone biosynthesis and to UbiX- and UbiD-like proteins from different microbial strains catalyzing the decarboxylation of various hydroxybenzoate compounds (Fig. 3) (30–33).

Heterologous expression studies in an *ubiX* null mutant of *E. coli* (Fig. 4 and 7) indicated that *slr1099* indeed codes for a

TABLE 1

Comparative analyses of chlorophyll, PQ and phylloquinone contents as well as the photosynthesis rates in *Synechocystis* sp. WT and knockout mutants cultivated in liquid culture

The data represent mean values and standard deviations of at least four independent sets of experiments.

	WT	*sll1797*::*aph*	*slr1099*::*aph*	*sll0936*::*aph*
Cells·10^7·A_{730}^{-1}	0.84 ± 0	2.52 ± 0.01	1.18 ± 0.07	1.91 ± 0.02
Chlorophyll (μg·A_{730}^{-1})	1.8 ± 0.51	1.3 ± 0.08	2.0 ± 0.63	2.4 ± 0.10
PQ (μg·A_{730}^{-1})	226 ± 15	8 ± 3	42 ± 16	67 ± 7
Phylloquinone (μg·A_{730}^{-1})	120 ± 16	117 ± 18	126 ± 17	119 ± 2
Photosynthesis rates (nmol O_2·s^{-1}·(μg of Chl) $^{-1}$)	17.9 ± 0.45	0.7 ± 0.57	16.5 ± 0.59	14.9 ± 0.29

4-hydroxy-3-prenylbenzoate decarboxylase. The enzyme was functionally expressed and compensated the defect in growth rate and in ubiquinone synthesis of the *E. coli* Δ*ubiX* mutant (Fig. 4). Like Sll0936, Slr1099 was predominantly found in the membrane fractions of *E. coli* (Fig. 5), whereas decarboxylase activity was detectable only in crude protein fractions harboring the recombinant Slr1099 protein. Perhaps separation of the soluble proteins from the membrane bound ones by high speed centrifugation (100,000 × *g*) removed a compound from the membranes and/or disturbed a membrane-associated complex required for the catalytic active conformation of the decarboxylase. Biochemical studies on *E. coli* described that protein complexes are involved in ubiquinone biosynthesis (38, 39), and it was suggested that 2-octaprenylphenol, the decarboxylase product, may play a critical role in stabilizing or activating the *O*-methyltransferase UbiG, a downstream enzyme in ubiquinone biosynthesis (40). Similarly, cyanobacteria may require protein complexes for PQ biosynthesis, and intermediates like 4-hydroxy-3-solanesylbenzoate and 2-solanesylphenol might be important for stabilizing proteins such as the decarboxylase (Fig. 1).

Despite intensive efforts, conclusive evidence for the catalytic activity of Sll0936 and UbiD could not be provided. The sequence homologies to UbiD like aromatic decarboxylases (Fig. 3), however, suggest that both proteins have decarboxylase activity. Our finding that UbiD expression did not restore ubiquinone biosynthesis in the *E. coli* Δ*ubiX* (results not shown) indicates that UbiX and UbiD have distinct roles in *E. coli*. This may also hold true for cyanobacteria, because similar results were obtained with the respective *Synechocystis* sp. proteins in complementation studies. The conflicting data regarding the generation of an *E. coli ubiD* null mutant (Refs. 11 and 35 and this study) suggest that *ubiD* is essential under certain conditions, and further investigations will be required to elucidate the role of UbiD in ubiquinone biosynthesis.

In *Synechocystis* sp., disruption of either *slr1099* or *sll0936* resulted in reduced growth rates and PQ contents, indicating that both genes are required for PQ biosynthesis (Fig. 9 and Table 1). Hence, the mutant phenotypes resembled those of the *E. coli* Δ*ubiX* and Δ*ubiD* mutants, which are impaired in ubiquinone biosynthesis (12, 18). According to the cell number/A_{730} ratio, a defect in PQ biosynthesis seems to affect also cell size/structure of the *Synechocystis* sp. mutants (Table 1). Although the very low PQ level in the *sll1797*::*aph* resulted in an almost complete loss of photosynthetic activity, PQ levels reduced to ~20% of the WT level appeared to be high enough for enabling photosynthetic electron transport in the *slr1099*::*aph* and *sll0936*::*aph* mutants in rates similar to those of the wild type (Table 1). The low PQ levels detected in the single-gene knock-out mutants of *Synechocystis* sp. might be caused by residual enzyme activity of the respective intact protein preserved in the single-gene knock-out mutants, which required interaction with the second decarboxylase for full activity in a similar way as suggested (18) with regard to UbiX and UbiD in *E. coli*. However, we cannot exclude the possibility that another, as yet unknown decarboxylase is present in *Synechocystis* sp.

Unlike the PQ content, inactivation of *slr1099*, *sll0936*, or *sll1779* had no impact on the content of phylloquinone (Table 1). The severe defect in PQ biosynthesis could not be remedied by phylloquinone in *Synechocystis* sp. as reported for higher plants (5, 41). Therefore, it can be concluded that PQ is the functionally most important prenylquinone in cyanobacterial electron transport pathways. PQ, on the other hand, was shown to partially complement the lack of phylloquinone in photosystem I of *Synechocystis* sp. and *Chlamydomonas reinhardtii* but not in *Arabidopsis thaliana* (42–44).

Altogether, our study indicates that during evolution, cyanobacterial ancestors modified their pre-existing ubiquinone biosynthetic pathway toward the production of PQ. Why was it advantageous to substitute ubiquinone by PQ? Oxygenic photosynthesis, as performed by cyanobacteria and plants, gives rise to the formation of reactive oxygen species, and the higher antioxidant activity of PQ in comparison to ubiquinone, as shown in an *in vitro* model system (45), may have allowed a better prevention of oxidative damage. The first three reaction steps of the cyanobacterial PQ biosynthetic pathway are nearly identical to those during ubiquinone biosynthesis in *E. coli*. Both pathways are initiated by a chorismate pyruvate-lyase; next the prenyl side chain is inserted by a 4-hydroxybenzoate prenyltransferase; and decarboxylases finally convert 4-hydroxy-3-prenylbenzoate to 2-prenylphenol (Fig. 10). Although in cyanobacteria 2-prenylphenol contains a solanesyl (nonaprenyl) side chain, it is synthesized with an octaprenyl side chain in *E. coli*. The 2-prenylphenol is converted to PQ or ubiquinone in a series of methylation and hydroxylation reactions at the aromatic head group (Fig. 10). For ubiquinone production, three C-hydroxylations, two *O*-methylations, and one C-methylation are required. In cyanobacteria, one C-hydroxylation and two C-methylations likely yield PQ (Fig. 1, Fig. 10). These reaction steps involve presumably enzymes with altered substrate specificities in comparison to the *E. coli* proteins for ubiquinone biosynthesis. Plants, on the other hand, synthesize PQ via a pathway that is, apart from the isoprenoid precursor, identical to the first reaction steps during vitamin E biosynthesis. The vitamin E biosynthetic pathway is conserved in cyanobacteria

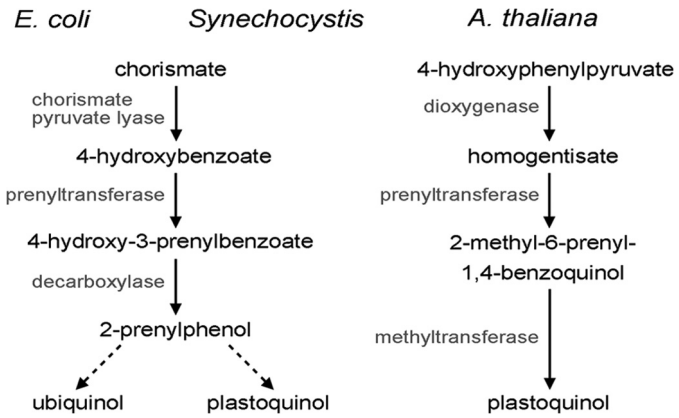

FIGURE 10. **The first steps of the PQ biosynthetic pathway in the cyanobacterium *Synechocystis* sp. in comparison to ubiquinone biosynthesis in the proteobacterium *E. coli* and PQ biosynthesis in the higher plant *A. thaliana*.** The *dashed arrows* indicate that further hydroxylation and methylation reaction steps are required for ubiquinone and PQ biosynthesis.

and plants. A 4-hydroxyphenylpyruvate dioxygenase converts 4-hydroxyphenylpyruvate to homogentisate, the aromatic precursor for PQ (Fig. 10). In the next step, a bifunctional prenyltransferase catalyzes the decarboxylation as well as the prenylation of homogentisate so that 2-methyl-6-solanesyl-benzoquinol is formed. This intermediate is finally converted to PQ by the activity of a methyltransferase (Fig. 10).

Acknowledgment—We gratefully acknowledge help from Stephan Buchkremer in the characterization of Slr1099.

REFERENCES

1. Schultze, M., Forberich, B., Rexroth, S., Dyczmons, N. G., Roegner M., and Appel, J. (2009) Localization of cytochrome b_6f complexes implies an incomplete respiratory chain in cytoplasmic membranes of the cyanobacterium *Synechocystis* sp. PCC6803. *Biochim. Biophys. Acta* **1787,** 1479–1485
2. Collins, M. D., and Jones D. (1981) Distribution of isoprenoid quinone structural types in bacteria and their taxonomic implications. *Microbiol. Rev.* **45,** 316–354
3. Scherer, S., Alpes, I., Sadowski, H., and Böger, P. (1988) Ferredoxin-$NADP^+$ oxidoreductase is the respiratory NADPH dehydrogenase of the cyanobacterium *Anabaena variabilis*. *Arch. Biochem. Biophys.* **267,** 228–235
4. Sadre, R., Frentzen, M., Saeed, M., and Hawkes, T. (2010) Catalytic reactions of the homogentisate prenyl transferase involved in plastoquinone-9 biosynthesis. *J. Biol. Chem.* **285,** 18191–18198
5. Cheng, Z., Sattler, S., Maeda, H., Sakuragi, Y., Bryant, D. A., and DellaPenna, D. (2003) Highly divergent methyltransferases catalyze a conserved reaction in tocopherol and plastoquinone synthesis in cyanobacteria and photosynthetic eukaryotes. *Plant Cell* **15,** 2343–2356
6. Dähnhardt, D., Falk, J., Appel, J., van der Kooij, T. A., Schulz-Friedrich, R., and Krupinska, K. (2002) The hydroxyphenylpyruvate dioxygenase from *Synechocystis* sp. PCC 6803 is not required for plastoquinone biosynthesis. *FEBS Lett.* **523,** 177–181
7. Sakuragi, Y., and Bryant, D. A. (2006) in *Photosystem I. The Light-Driven Plastocyanin. Ferredoxin Oxidoreductase* (Golbeck, J. H., ed) pp. 205–222, Springer, Dordrecht, The Netherlands
8. Sadre, R., Pfaff C., and Buchkremer, S. (2012) Plastoquinone-9 biosynthesis in cyanobacteria differs from that in plants and involves a novel 4-hydroxybenzoate solanesyltransferase. *Biochem. J.* **442,** 621–629
9. Ashby, M. N., and Edwards, P. A. (1990) Elucidation of the deficiency in two yeast coenzyme Q mutants. Characterization of the structural gene encoding hexaprenyl pyrophosphate synthetase. *J. Biol. Chem.* **265,** 13157–13164
10. Rippka, R. (1988) Isolation and purification of cyanobacteria. *Methods Enzymol.* **167,** 3–27
11. Baba, T., Ara, T., Hasegawa, M., Takai, Y., Okumura, Y., Baba, M., Datsenko, K. A., Tomita, M., Wanner, B. L., and Hirotada Mori (2006) Construction of *Escherichia coli* K-12 in-frame, single-gene knockout mutants. The Keio collection. *Mol. Syst. Biol.* 2006.0008
12. Cox, G. B., Young, I. G., McCann, L. M., and Gibson, F. (1969) Biosynthesis of ubiquinone in *Escherichia coli* K-12 location of genes affecting the metabolism of 3-octaprenyl-4-hydroxybenzoic acid and 2-octaprenylphenol. *J. Bacteriol* **99,** 450–458
13. Monod, J., Cohen-Bazire, S., and Cohn, M. (1951) Sur la biosynthèse de la *p*-galactosidase (lactase) chez *Escherichia coli.* La spécificité de l'induction. *Biochim. Biophys. Acta* **7,** 585–599
14. Datsenko, K. A., and Wanner, B. L. (2000) One-step inactivation of chromosomal genes in *Escherichia coli* K-12 using PCR products. *Proc. Natl. Acad. Sci. U.S.A.* **97,** 6640–6645
15. Link, A. J., Phillips, D., and Church, G. M. (1997) Methods for generating precise deletions and insertions in the genome of wild-type *Escherichia coli*. Application to open reading frame characterization. *J. Bacteriol.* **179,** 6228–6237
16. Nakao, M., Okamoto, S., Kohara, M., Fujishiro, T., Fujisawa, T., Sato, S., Tabata, S., Kaneko, T., and Nakamura, Y. (2010) CyanoBase. The cyanobacteria genome database update 2010. *Nucleic Acids Res.* **38,** D379–D381
17. Chomczynski, P., and Sacchi, N. (1987) Single-step method of RNA isolation by acid guanidinium thiocyanate-phenol-chloroform extraction. *Anal. Biochem.* **162,** 156–159
18. Gulmezian, M., Hyman, K. R., Marbois, B. N., Clarke, C. F., and Javor, G. T. (2007) The role of UbiX in *Escherichia coli* coenzyme Q biosynthesis. *Arch. Biochem. Biophys.* **467,** 144–153
19. Williams, J. G. (1988) Construction of specific mutations in photosystem II photosynthetic reaction center by genetic engineering methods in *Synechocystis* 6803. *Methods Enzymol.* **167,** 766–778
20. Bradford, M. M. (1976) A rapid and sensitive method for the quantitation of microgram quantities of protein utilizing the principle of protein-dye binding. *Anal. Biochem.* **72,** 248–254
21. Lichtenthaler, H. K. (1987) Chlorophyll and carotenoids pigments of photosynthetic biomembranes. *Methods Enzymol.* **148,** 350–382
22. Aravind, L., and Anantharaman, V. (2003) HutC/FarR-like bacterial transcription factors of the GntR family contain a small molecule-binding domain of the chorismate lyase fold. *FEMS Microbiol. Lett.* **222,** 17–23
23. Altschul, S. F., Madden, T. L., Schäffer, A. A., Zhang, J., Zhang, Z., Miller, W., and Lipman, D. J. (1997) Gapped BLAST and PSI-BLAST. A new generation of protein database search programs. *Nucleic Acids Res.* **25,** 3389–3402
24. Quevillon, E., Silventoinen, V., Pillai, S., Harte, N., Mulder, N., Apweiler, R., and Lopez, R. (2005) InterProScan. Protein domains identifier. *Nucleic Acids Res.* **33,** W116–W120
25. Marchler-Bauer, A., Lu, S., Anderson, J. B., Chitsaz, F., Derbyshire, M. K., DeWeese-Scott, C., Fong, J. H., Geer, L. Y., Geer, R. C., Gonzales, N. R., Gwadz, M., Hurwitz, D. I., Jackson, J. D., Ke, Z., Lanczycki, C. J., Lu, F., Marchler, G. H., Mullokandov, M., Omelchenko, M. V., Robertson, C. L., Song, J. S., Thanki, N., Yamashita, R. A., Zhang, D., Zhang, N., Zheng, C., and Bryant, S. H. (2011) CDD. A Conserved Domain Database for the functional annotation of proteins. *Nucleic Acids Res.* **39,** D225–D229
26. Boratyn, G. M., Schäffer, A. A., Agarwala, R., Altschul, S. F., Lipman, D. J., and Madden, T. L. (2012) Domain enhanced lookup time accelerated BLAST. *Biol Direct.* **7,** 12
27. Larkin, M. A., Blackshields, G., Brown, N. P., Chenna, R., McGettigan, P. A., McWilliam, H., Valentin, F., Wallace, I. M., Wilm, A., Lopez, R., Thompson, J. D., Gibson, T. J., and Higgins, D. G. (2007) Clustal W and Clustal X version 2.0. *Bioinformatics* **23,** 2947–2948
28. Tamura, K., Peterson, D., Peterson, N., Stecher, G., Nei, M., and Kumar, S. (2011) MEGA5. Molecular evolutionary genetics analysis using maximum likelihood, evolutionary distance, and maximum parsimony methods. *Mol. Biol. Evol.* **28,** 2731–2739
29. Smith, N., Roitberg, A. E., Rivera, E., Howard, A., Holden, M. J., Mayhew,

M., Kaistha, S., and Gallagher, D. (2006) Structural analysis of ligand binding and catalysis in chorismate lyase. *Arch. Biochem. Biophys.* **445,** 72–80
30. Rangarajan, E. S., Li, Y., Iannuzzi, P., Tocilj, A., Hung, L. W., Matte, A., and Cygler, M. (2004) Crystal structure of a dodecameric FMN-dependent UbiX-like decarboxylase (Pad1) from *Escherichia coli* O157:H7. *Protein Sci.* **13,** 3006–3016
31. Liu, J., Zhang, X., Zhou, S., and Tao, P. (2007) Purification and Characterization of a 4-Hydroxybenzoate Decarboxylase from *Chlamydophila pneumoniae* AR39. *Curr. Microbiol.* **54,** 102–107
32. Matsui, T., Yoshida, T., Hayashi, T., and Nagasawa, T. (2006) Purification, characterization, and gene cloning of 4-hydroxybenzoate decarboxylase of *Enterobacter cloacae* P240. *Arch. Microbiol.* **186,** 21–29
33. Lupa, B., Lyon, D., Gibbs, M. D., Reeves, R. A., and Wiegel, J. (2005) Distribution of genes encoding the microbial non-oxidative reversible hydroxyarylic acid decarboxylases/phenol carboxylases. *Genomics* **86,** 342–351
34. Lupa, B., Lyon, D., Shaw, L. N., Sieprawska-Lupa, M., and Wiegel, J. (2008) Properties of the reversible nonoxidative vanillate/4-hydroxybenzoate decarboxylase from *Bacillus subtilis*. *Can. J. Microbiol.* **54,** 75–81
35. Liu, J., and Liu, J. H. (2006) Ubiquinone (Coenzyme Q) biosynthesis in *Chlamydophila pneumoniae* AR39. Identification of the ubiD gene. *Acta Biochim. Biophys. Sin.* **38,** 725–730
36. Krogh, A., Larsson, B., von Heijne, G., and Sonnhammer, E. L. (2001) Predicting transmembrane protein topology with a hidden Markov model. Application to complete genomes. *J. Mol. Biol.* **305,** 567–580
37. Siebert, M., Severin, K., and Heide, L. (1994) Formation of 4-hydroxybenzoate in *Escherichia coli*. Characterization of the *ubiC* gene and its encoded enzyme chorismate pyruvate-lyase. *Microbiology.* **140,** 897–904
38. Leppik, R. A., Stroobant, P., Shineberg, B., Young, I. G., and Gibson, F. (1976) Membrane-associated reactions in ubiquinone biosynthesis. *Biochim. Biophys. Acta* **428,** 146–156
39. Knöll, H. E. (1979) Isolation of a soluble enzyme complex comprising the ubiquinone-8 synthesis apparatus from the cytoplasmatic membrane of *Escherichia coli*. *Biochem. Biophys. Res. Commun.* **91,** 919–925
40. Gulmezian, M., Zhang, H., Javor, G. T., and Clarke, C. F. (2006) Genetic evidence for an interaction of the UbiG *O*-methyltransferase with UbiX in *Escherichia coli* coenzyme Q biosynthesis. *J. Bacteriol.* **188,** 6435–6439
41. Tian, L., DellaPenna, D., and Dixon, R. A. (2007) The pds2 mutation is a lesion in the *Arabidopsis* homogentisate solanesyltransferase gene involved in plastoquinone biosynthesis. *Planta* **226,** 1067–1073
42. Johnson, T. W., Shen, G., Zybailov, B., Kolling, D., Reategui, R., Beauparlant, S., Vassiliev, I. R., Bryant, D. A., Jones, A. D., Golbeck, J. H., and Chitnis, P. R. (2000) Recruitment of a foreign quinone into the A_1 site of photosystem I. I. Genetic and physiological characterization of phylloquinone biosynthetic pathway mutants in *Synechocystis* sp. PCC 6803. *J. Biol. Chem.* **275,** 8523–8530
43. Shimada, H., Ohno, R., Shibata, M., Ikegami, I., Onai, K., Ohto, M. A., and Takamiya, K. (2005) Inactivation and deficiency of core proteins of photosystems I and II caused by genetical phylloquinone and plastoquinone deficiency but retained lamellar structure in a T-DNA mutant of *Arabidopsis*. *Plant J.* **41,** 627–637
44. Lefebvre-Legendre, L., Rappaport, F., Finazzi, G., Ceol, M., Grivet, C., Hopfgartner, G., and Rochaix J. D. (2007) Loss of phylloquinone in *Chlamydomonas* affects plastoquinone pool size and photosystem II synthesis. *J. Biol. Chem.* **282,** 13250–13263
45. Kruk, J., Jemiola-Rzeminska, M., and Strzalka, K. (1997) Plastoquinol and α-tocopherol quinol are more active than ubiquinol and α-tocopherol in inhibition of lipid peroxidation. *Chem. Phys. Lipids* **87,** 73–80